

A MICRO TRANSLATING LENS UNIT FOR STEREO IMAGING THROUGH SINGLE-IMAGE ENDOSCOPE

Wook Choi¹, Gennady Sigal², Vladimir Rubtsov², and Chang-Jin "CJ" Kim¹

¹Mechanical and Aerospace Engineering Department, University of California, Los Angeles (UCLA)

²Intelligent Optical Systems, Inc. (IOS), Torrance, California, USA

ABSTRACT

Most stereo imaging tools require the use of multiple optical channels to achieve slightly different viewing angles around an object of interest, which inevitably increases overall size and structural complexity compared to single imaging systems. In this study, a translating lens device is developed to generate stereo images especially for endoscopic applications through a single-objective lens setup. A silicon comb-drive translates a miniature lens across the optical axis in front of an optical circuit to create different viewing angles through a single optical channel. Up to $\pm 50 \mu\text{m}$ of lens translation has been tested at 24 V_{DC} providing stereo acquisition for 3D perception. Coupling 3D viewing capability and the size advantage of a single endoscopic optical system, this technology aims to enhance the operator's visual perception without sacrificing the endoscope's size.

INTRODUCTION

Stereo imaging is widely used these days to provide viewers with 3D perception in many different applications including medical, academic, and cinema [1-3]. Stereo image capturing devices used for such 3D effects mostly use multiple optical channels to achieve different object-viewing angles. To avoid the use of such multiple optical systems, which complicates lens configurations and increases overall system size, various stereo methods using a single optical system have been introduced [4]. Using one such method [5], we have previously reported development of a device, miniaturized through microfabrication [6], aimed at endoscopic applications. At resonance, the disc-flipping device in [6], whose time-consuming fabrication included molding of a Pyrex[®] disc, generated image disparities large enough for distance measurement but not satisfactory for general 3D perception.

In this study, we propose a new single-lens stereo imaging mechanism, featuring (1) non-resonating device operation, which does not require the high-speed image processor of [6], (2) simple fabrication process involving only silicon micromachining, (3) image shift large enough for 3D viewing, and (4) a simple endoscopic optical circuit, which uses a minimal number of lenses.

PRINCIPLE

Figure 1 illustrates the stereo imaging principle for the proposed approach. A simple de-centering of a lens generates image shifts of the objects seen through the lens. When the lens center is on the optical axis as in Figure 1 (a), images of the objects behind the lens are reversed and aligned under the optical axis. If the lens translates upward as in Figure 1 (b), images of the objects also move up.

However, the amount of image shift for each object varies based on its physical distance from the lens. That is, the image of a closer object shifts more than that of a farther one. If the lens translates downward as in Figure 1 (c), the images move down, and the shifting amounts are again based on the distances of the objects from the lens. The proposed mechanism utilizes this relationship between the object distance and the image shift to generate different viewing angles for 3D perception. Comparing the amount of image shift with pre-calibrated data, the system can further estimate how far away each object is.

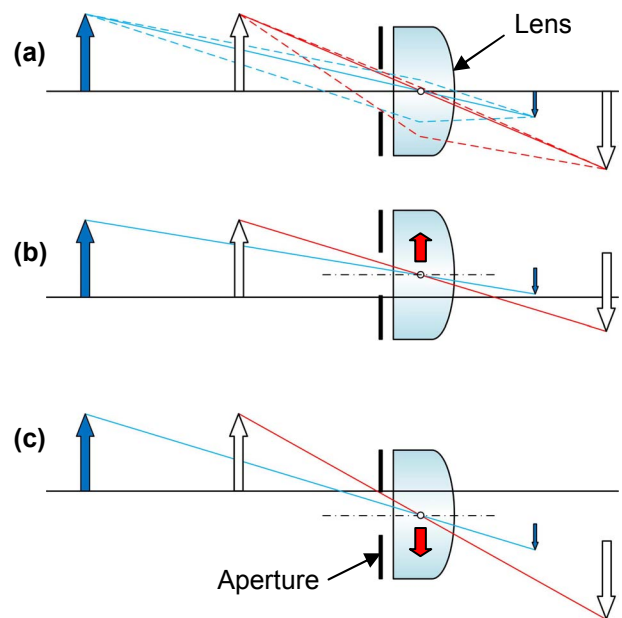


Figure 1: Stereo image generation by de-centering of the lens. (a) When the lens center is on the optical axis, images of the two objects (arrows) have their bases on the optical axis. When the lens moves (b) upward or (c) downward, images of the objects behind the lens all move up or down, relatively. However, the amounts of image translations are dependent on how close the objects are to the lens. Images of closer objects shift more than those of farther objects.

Figure 2 illustrates the proposed stereo imaging principle in more detail to verify and estimate the image shift. At the initial position of the solid-lined lens, an object of height \overline{Ab} projects an image of height $\overline{A'b'}$ behind the lens. If the lens translates downward (shown with dotted-lines) by δ , the tip of the image moves from A' to A'' . If the magnification is γ , the size of each projected image can be estimated by the following equations:

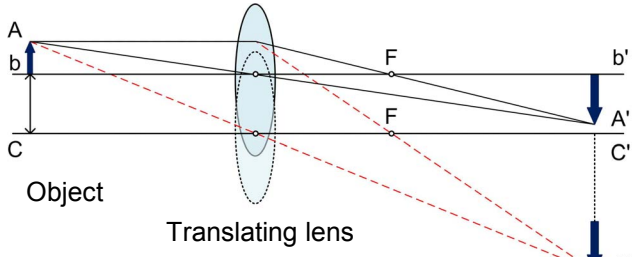


Figure 2: Image shift by lens translation. The total image shift by the lens translation δ in this illustration is $A'A''$. This image shift becomes larger if the magnification of the lens is greater.

$$\begin{aligned} \overline{A'b'} &= \overline{Ab} \times \gamma \\ \overline{A''C'} &= (\overline{Ab} + \delta) \times \gamma \end{aligned} \quad (1)$$

Then the overall image shift Δ is calculated by,

$$\begin{aligned} \Delta &= \overline{A''b'} - \overline{A'b'} = (\overline{A''C'} + \delta) - (\overline{Ab} \times \gamma) \\ &= \left[\{(\overline{Ab} + \delta) \times \gamma\} + \delta \right] - (\overline{Ab} \times \gamma) \\ &= \delta \times (\gamma + 1) \end{aligned} \quad (2)$$

Equation (2) explains that the amount of image shift Δ depends on the lens translating distance δ and the image magnification γ , the latter of which is related to the object distance. Assuming that a lens unit consisting of a $500 \mu\text{m}$ diameter aperture and a 2 mm focal length plano-convex lens translates $\pm 50 \mu\text{m}$ across the optical axis, Figure 3 simulates the image shifts for varying object distances for two cases: the imaging plane located 2.4 mm or 3 mm behind the lens (focusing point: 10 mm or 5 mm in front of the lens, respectively). The result verifies that the principal ray shifts more if the object is closer to the lens or the imaging plane is farther from the lens (i.e., the gap "D" in Figure 3 is larger). This optical simulation was run for the object distance in the range of $3\text{-}30 \text{ mm}$, which is practical for endoscopic applications. Additional optical simulations suggested good optical quality for the given lens unit and its translation range.

TEST SETUP

Because the stereo imaging plan in this study is mainly for endoscopic applications, an optical fiber-based circuit with minimal use of lenses has been built for the imaging test. Figure 4 (top) illustrates the stereo imaging device integrated with the endoscopic optical circuit consisting of an imaging fiber bundle, transducer lens, and a CCD camera connected to the control computer. A lens unit packaged in the translating system is located in front of the imaging fiber bundle, which passes the images to the CCD camera through the transducer lens. The translation of the lens is achieved by the two sets of silicon comb drive actuators of the lens shuttle, as shown in the simplified drawing in Figure 4 (bottom). This lens shuttle is suspended by two folded spring fixtures (not shown in the drawing) to facilitate the translation.

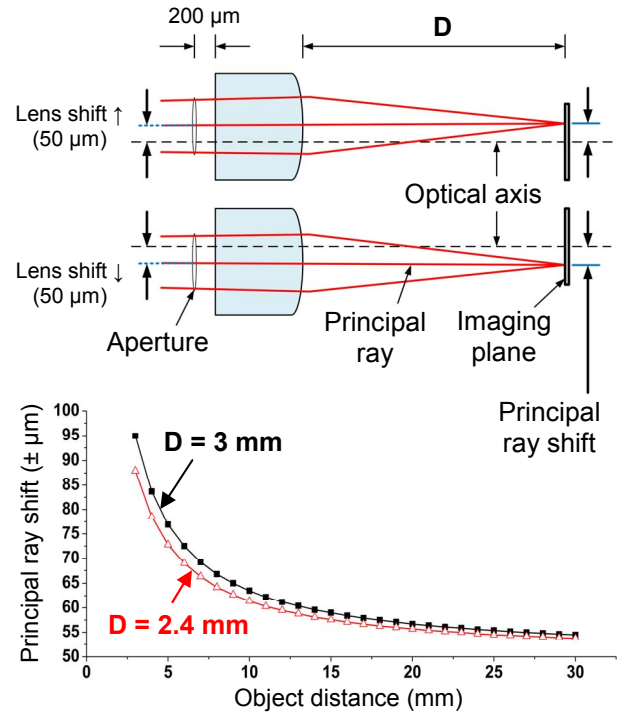


Figure 3: Optical simulation results to find the principal ray shift by lens translation. (Top) A lens of 2 mm focal length bundled with an aperture $500 \mu\text{m}$ in diameter in the front is assumed to de-center $\pm 50 \mu\text{m}$. (Bottom) Principal ray shifts showing dependence on (1) the object distance and (2) focusing distance. The shift becomes larger as the object is closer or the gap between the lens and the imaging plane ("D") is larger (for a shorter focusing distance).

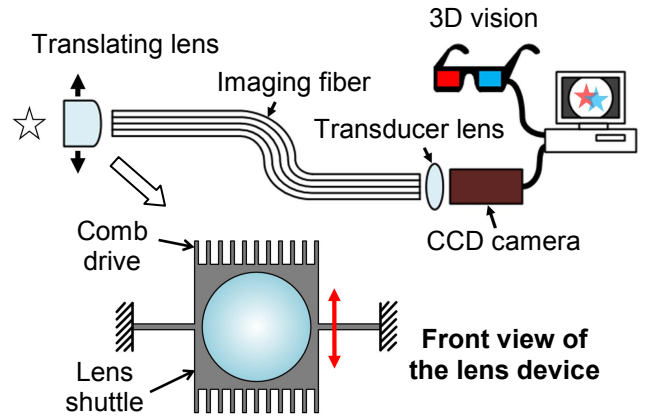


Figure 4: Illustration of the stereo imaging setup. Translating lens unit, driven by two sets of electrostatic comb actuators, is implemented with an endoscopic optical circuit.

A computer system synchronizes the camera with the driving electric signal to capture the images shifted at the extreme lens locations, and also separates the images into two real-time streams for 3D viewing or object distance measurement.

FABRICATION AND OPERATION

Fabrication process

Figure 5 shows the fabrication process for the stereo

shuttle device (left), which will translate the lens unit, and its aperture structure (right). An SOI (50 μm -thick Si device / 0.5 μm -thick buried oxide / 350 μm -thick Si handle layer) wafer is used as the substrate as shown in Figure 5 (a). To eliminate additional electrode deposition and patterning, a heavily doped Si device layer of the SOI is chosen. First, the bottom handle layer of the SOI is anisotropically etched by DRIE, followed by exposed buried oxide removal by RIE as in Figure 5 (b). The device layer of the SOI is then patterned by DRIE to form the comb drive actuators on the shuttle device and to make a hole 500 μm in diameter on the aperture structure, shown in Figure 5 (c). The shuttle device is released at the same time in this step. A plano-convex lens (NT65-253, Edmund Optics, NJ, USA) 1 mm in diameter and 800 μm in thickness is inserted into the fabricated aperture structure with a 150 μm -thick ring spacer in between to ensure the proper gap between the lens and the aperture. This lens has an effective focal length of 2 mm as in the optical simulation in the previous section. As the last step, the assembled lens unit is inserted in the silicon shuttle, as in Figure 5 (d). The device is 10 mm \times 10 mm in overall dimension.

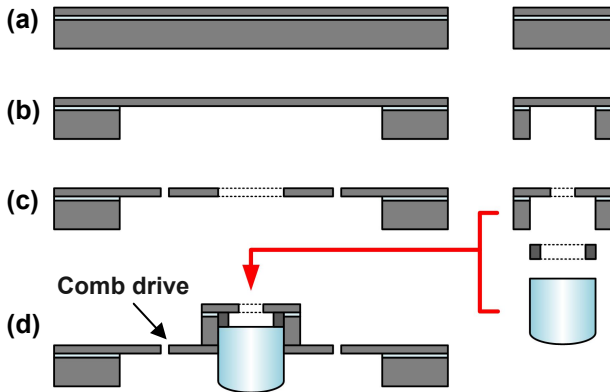


Figure 5: Fabrication of the stereo device. (a-c, left) Process flow for translating silicon shuttle. (a-c, right) Process flow for the aperture screen and its assembly with a plano-convex lens 1 mm in diameter and 800 μm in thickness and a ring spacer. (d) The assembled lens unit is inserted in the shuttle.

Device operation

Figure 6 (left) shows the photo of the finally assembled device with wires glued on the device surfaces with silver paint to ensure electrical connections. For this device, folded springs with 1 mm in length, 5 μm in width, and 50 μm in thickness are used to suspend the lens shuttle. Each comb drive actuator consists of 700 pairs of interdigitated fingers each 120 μm in length, 5 μm in width, and 50 μm in thickness. The gap between the opposing fingers is 3 μm . The stationary and moving fingers have 10 μm of overlap when no electric potential is applied. When 24 V_{DC} is applied between the stationary and moving comb sides, up to 50 μm of shuttle translation was achieved, as shown in the microscopic photo in Figure 6 (right). The translation was measured under the microscope using the patterned gauge located directly adjacent to the comb drive.

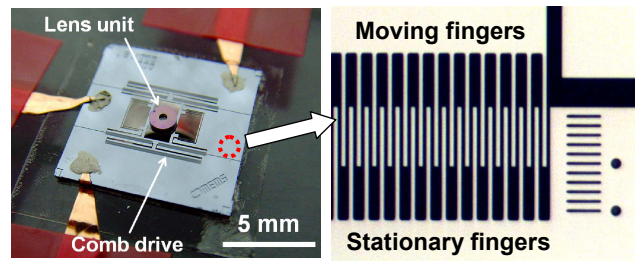


Figure 6: Fabricated lens-translating stereo device (left) and a microscopic view of its comb drive operation (right). The lens shuttle, suspended by four 1 mm-long folded-beam springs, translates $\pm 50 \mu\text{m}$ with 24 V_{DC} applied alternately to the two sets of comb drives.

IMAGING TEST

Stereo for 3D viewing

A plastic pipette tip approximately 3 cm long is used as a target object for the stereo imaging test using the fabricated lens translation device aligned in front of the endoscopic optical circuit. Figure 7 shows the stereo images generated by the lens translation. As the lens translates approximately $\pm 50 \mu\text{m}$ at 24 V_{DC} as explained in the previous section, the image of the target object shifts in the same direction as the lens' translation (Figure 7 (a-1) and (a-2)). The entire image of the target translates more than $\pm 50 \mu\text{m}$, but the image of the closer part (the tip of the pipette tip) moves more than that of the faraway part (the base of the pipette tip), as predicted by the simulation result in Figure 3 when the lens is focused for 5 mm length. In Figure 7 (b), the two captured images have been aligned to a stationary reference point so that only their relative shift can be seen. Two points – one each in Figures 7 (a-1) and (a-2), that represent an identical spot on the pipette tip's base are used as the common reference point. As a result, the two images in Figure 7 (b) have a disparity near the target's tip area while the base area is kept unmoved, i.e., the object appears tilted between the two images. Using superimposed and color-converted images from Figure 7 (b), Figure 7 (c) presents the anaglyph stereo image, providing 3D perception of the target object to the viewer wearing red/cyan anaglyphic glasses (i.e., the pipette tip appears to be protruding out of the page).

Stereo for distance measurement

Figure 8 shows the object distance measurement by the endoscopic lens translation system using the same pipette tip as in the previous test. The object tip is 10 mm away from the device and is focused upon by the lens. Therefore, the gap between the lens and the imaging fiber is 2.4 mm ("D" in Figure 3), and the image shift vs. distance follows the lower curve in the graph in Figure 3. The LabVIEW-based shift-detecting program detects the shifts at the edge area and converts them into a distance. As shown in Figure 8, it successfully measured the distance to the object as it was moved closer to the lens device.

CONCLUSION

The stereo imaging device introduced in this study is

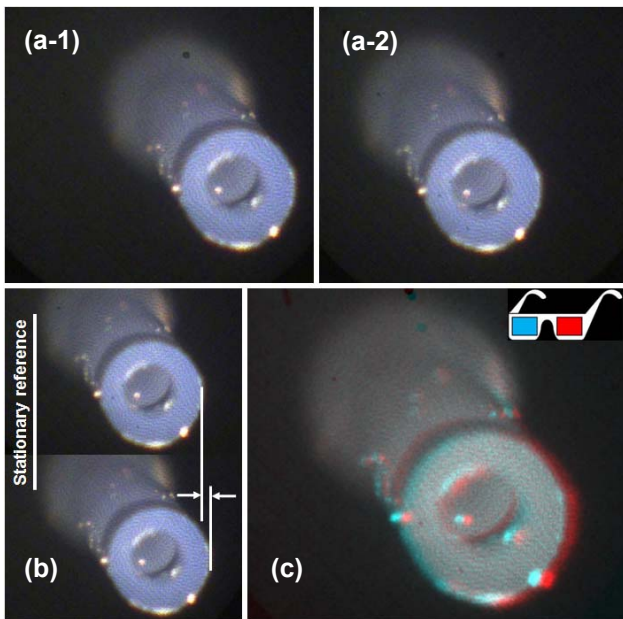


Figure 7: Object image tilting for 3D viewing. A 3 cm-long pipette tip is used as the target object. (a-1) and (a-2) As the lens unit translates $\pm 50 \mu\text{m}$, the shift of the object image is observed. (b) Arranged images of (a-1) and (a-2) to show only the distance-dependent image shift. Such a difference in shift tilts the object image about an axis in the page plane, resulting in the different viewing angles, i.e., 3D perception, to the observer. (c) An anaglyph image formed by superimposing red and cyan images of (b) for stereo viewing.

mainly designed to have large enough image shift to make 3D viewing possible, while avoiding the complications of the existing stereo methods and their implementation. With an actively moving lens unit in front of the imaging fiber bundle, this stereo method has shown promise for 3D viewing and distance measurement in various endoscopic applications if electrical wiring is allowed for lens operations. Our next task is to integrate a further miniaturized device with a real endoscope less than 1 cm in diameter for inspection in confined hard-to-reach spaces.

ACKNOWLEDGEMENTS

The authors thank Mr. Michael Levin for his help on the imaging test and experiment setup, and Mr. James Jenkins for valuable discussions about the visualization and composition of the manuscript. The software program to detect the image shift was developed by Dr. Alex Berger. The signal generator synchronized to the camera was developed by Mr. Stephen Pflanze.

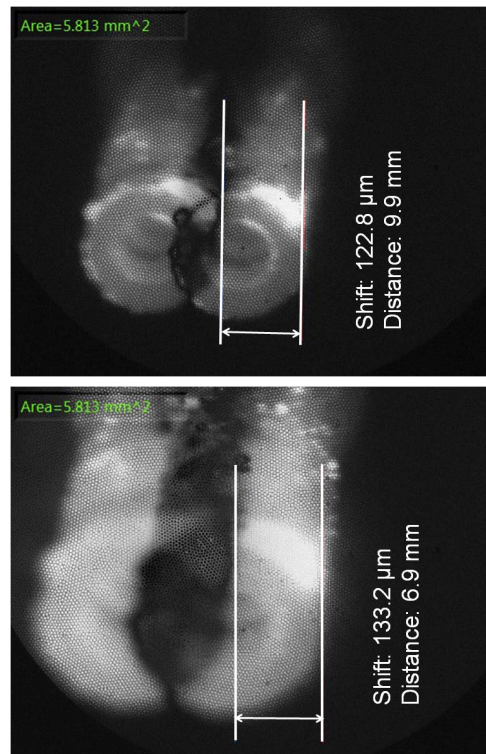


Figure 8: Distance measurement by lens translation. Two captured images are added together to find the shifted edges. A contrast difference allows the detection of the image shift. (Top) When the object is 10 mm away from the device, and (Bottom) when the object is moved closer to the device (7 mm away).

REFERENCES

- [1] A. F. Durrani and G. M. Preminger, "Three-dimensional video imaging for endoscopic surgery", *Computers in Biology and Medicine*, vol. 25, pp. 237-247, 1995.
- [2] H. W. Schreier, D. Garcia and M. A. Sutton, "Advances in light microscope stereo vision," *Experimental Mechanics*, vol. 44, pp. 278-288, 2004.
- [3] L. Lipton, "Foundations of the Stereoscopic Cinema," *Van Nostrand Reinhold*, New York, 1982.
- [4] A. Goshtasby and W. A. Gruver, "Design of a single-lens stereo camera system", *Pattern Recognition*, vol. 26, pp. 923-937, 1993.
- [5] Y. Nishimoto and Y. Shirai, "A feature-based stereo model using small disparities," in *Proceedings of the IEEE International Workshop on Industrial Applications of Machine Vision and Machine Intelligence. Seiken Symposium*, pp. 192-196, Tokyo, Japan, Feb. 1987.
- [6] W. Choi, M. Akbarian, V. Rubtsov, and C.-J. Kim, "Microfabricated flipping glass disc for stereo imaging in endoscopic visual inspection," in *Proceedings of IEEE International Conference on MEMS*, pp. 160-163, Sorrento, Italy, Jan. 2009.